Integer and Fractional Quantum Hall Effect

Niraj Venkat
(Dated: January 19, 2022)

The quantum Hall effect has made a lasting impact after it's experimental discovery forty years ago. Since then mathematics and physics have shown deep connections in the attempts to explain it. In this paper, we review the history of this famous effect named after Edwin Hall, who showed that applying a magnetic field perpendicular to a current-carrying metal strip causes a transverse voltage. We then discuss the integer quantum Hall effect discovered nearly a century later, and its trademark plateaus in conductance that allow us to estimate fundamental physical constants to incredible accuracy. Mathematical invariants provide a compelling theoretical framework for the integer conductance. We cover the fractional quantum Hall effect, and explain its ground and excited states. We conclude with the composite fermion picture that serves to unite the quantum Hall effect.

I. Introduction

A. Classical Charged Particle and Hall effect

We examine a particle of mass m and charge q in a uniform magnetic field in the z-direction $\mathbf{B} = (0, 0, B_z)$ restricted to move in the x-y plane with velocity $\mathbf{v}$. This obeys the classical Lorentz force law [1]:

$$m\frac{d\mathbf{v}}{dt} = \frac{q}{c}\mathbf{v} \times \mathbf{B} \quad (1)$$

Because $\mathbf{B}$ and $\mathbf{v}$ are perpendicular, the particle undergoes circular motion. Equating (1) to a centripetal force gives us an expression for the angular *cyclotron* frequency $\omega_c =$ [2]:

$$F = q\frac{v}{c}B_z = m\frac{v^2}{r} \implies \omega_c = \frac{v}{r} = \frac{qB_z}{mc} \quad (2)$$

While this describes a free particle in our $\mathbf{B}$ field fairly well, we are specifically interested in electrons confined to a more realistic environment like a material, which could be a conductor or insulator.

We now turn to the classical Hall effect shown here, discovered in 1879 by mathematician Edwin E. Hall [3]:

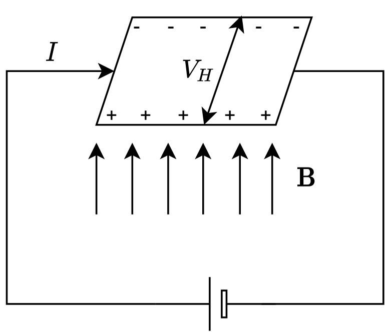

Figure 1: Classical Hall effect with Hall voltage V_H

To explain this we consider the *Drude model* which allows the electron to be influenced by an additional electric field $\mathbf{E}$ that can act on our particle in the absence of $\mathbf{B}$, as well as a frictional term which captures any impedence in our material, like impurities and other electrons [4]:

$$m\frac{d\mathbf{v}}{dt} = \frac{q}{c}\mathbf{v} \times \mathbf{B} + q\mathbf{E} - \frac{m\mathbf{v}}{\tau} \quad (3)$$

where τ is the scattering time, or average time between collisions. We then carry out the following substitutions:

- Use the convention for electrons $q = -e$
- In a steady-state equilibrium we set $d\mathbf{v}/dt = 0$
- Use current density $\mathbf{J} = -de\mathbf{v}$, where d is is the density of charge carriers

This lets us arrive at a matrix equation:

$$\begin{pmatrix} 1 & \omega_c\tau \\ -\omega_c\tau & 1 \end{pmatrix}\mathbf{J} = \sigma_{DC}\mathbf{E} \quad \text{where} \quad \sigma_{DC} = \frac{e^2 d\tau}{m} \quad (4)$$

Inverting the matrix equation (4) gives us a reformulation of the familiar *Ohm's law*: $\mathbf{J} = \sigma\mathbf{E}$ where σ is a proportionality constant called *conductivity* and σ_{DC} is the DC conductivity in the absence of a magnetic field. As the experiment in Fig. 1 shows, the electron has two degrees of freedom requiring σ to be represented by a *conductivity tensor*, specifically the matrix:

$$\sigma = \begin{pmatrix} \sigma_{xx} & \sigma_{xy} \\ -\sigma_{xy} & \sigma_{xx} \end{pmatrix} = \frac{\sigma_{DC}}{1 + \omega_c^2\tau^2}\begin{pmatrix} 1 & -\omega_c\tau \\ \omega_c\tau & 1 \end{pmatrix} \quad (5)$$

The *resistivity*, defined as inverse of conductivity, in the Drude model is given by:

$$\rho = \sigma^{-1} = \begin{pmatrix} \rho_{xx} & \rho_{xy} \\ -\rho_{xy} & \rho_{xx} \end{pmatrix} = \frac{1}{\sigma_{DC}}\begin{pmatrix} 1 & \omega_c\tau \\ -\omega_c\tau & 1 \end{pmatrix} \quad (6)$$

The diagonal elements in (5), (6) are identical due to rotational invariance in the x-y plane, whereas the off-diagonal terms are directly responsible for the Hall effect. The explanation is that we start off with $\mathbf{E}$ in the x-direction, after which turning on $\mathbf{B}$ causes the electrons to undergo cyclotron motion which induces a buildup of charge on one side of the metal strip, giving us the Hall voltage V_H in the y-direction. So far, we have had no application of quantum mechanics but this will change when we look at the quantum Hall effect.

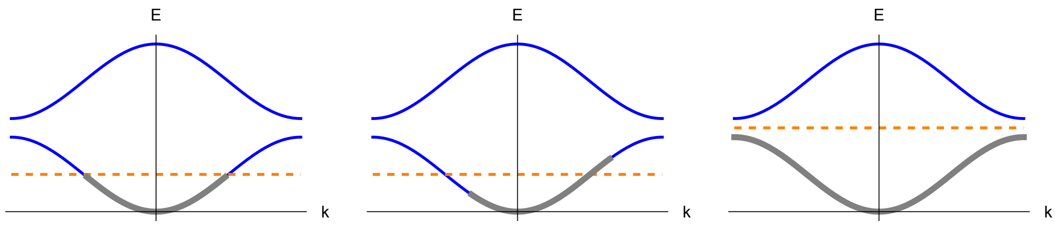

Figure 2: Brillouin zones with dashed line showing Fermi energy E_F. Left: Conductor, Middle: Conductor with charge carriers moving in the $+k$-direction due to applied electric field, Right: Insulator with no charge mobility due to completely filled band.

B. Solid State Physics

Moving to a different viewpoint called the *tight-binding model*, if we only allow electrons to occupy locations on a lattice, i.e. discretize space, then we find momentum becomes periodic. This also turns out to be conversely true, because they are Fourier transforms of each other. The one-dimensional lattice states have the wavefunction $\psi_n = e^{ikna}/\sqrt{N}$ and $\psi_{n\pm1} = e^{ika}\psi_n$ where n is the label of a lattice point, N is the total number of points and a is the lattice constant (distance between two neighbors). The set of solutions are invariant to $k \to k + \frac{2\pi}{a}$, so the wavenumber $k \in \left[-\frac{\pi}{a}, +\frac{\pi}{a}\right)$ is periodic. This range of momenta is known as the *Brillouin zone* (BZ).

For a one-dimensional lattice, the BZ has the topology of a circle $\mathbf{S}^1$. For a d-dimensional lattice, the BZ topology is the product of d circles, namely a torus $\mathbf{T}^d$. The one-dimensional BZ is shown in Fig. 2, which highlights the differences between conductors and insulators in the tight-binding picture.

If our particle in a magnetic field is restricted to x-y plane as before, then momentum/wavenumber $k_z = 0$. We recall that the Landau gauge gives our particle zero scalar potential Φ, and vector potential $\mathbf{A}$ can be chosen to be either $(-B_z y, 0, 0)$ or $(0, B_z x, 0)$. Both choices of gauge equivalently result in a harmonic oscillator Hamiltonian. Since $k_x, k_y \in \mathbb{R}$ range continuously, we have the infinitely degenerate energy spectrum $E_n = \hbar\omega_c(n + \frac{1}{2})$. Regarding the the metal strip in Fig. 1, we have a finite sample of area $A = L_x L_y$ so we get an $\mathcal{N}$-fold degeneracy in each Landau level which brings in the *flux quantum* Φ_0:

$$\mathcal{N} = \frac{q}{c}\frac{BA}{2\pi\hbar} = \frac{BA}{\Phi_0} \quad \text{where} \quad \Phi_0 = \frac{2\pi\hbar c}{q} \tag{7}$$

When deciding the Landau level ν, the electron must obey the restriction shown in Fig. 3. This quantization of the Landau levels will be useful in discussing the integer quantum Hall effect.

C. Spectral Flow and Berry Holonomy

In 1959, Aharonov and Bohm showed that electromagnetic gauge potentials are fundamental and the fields – even if they equal zero – are an emergent property. To understand this, we consider an experimental setup of a charged particle moving in a ring of radius r around a solenoid of radius a, carrying a magnetic field $\mathbf{B}$. Stokes' theorem (applied in Maxwell's equation) says that the line integral of vector potential $\mathbf{A}$ around a closed loop equals the enclosed magnetic flux.

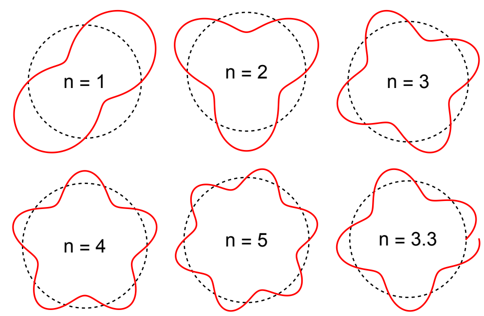

Figure 3: Integer values generate circular orbits compatible with the de Broglie wavelength of the electron. All orbits except bottom right are allowed. The energy of the particle depends on how many wavelengths sit in its orbit.

Choosing cylindrical coordinates, we have an angular dependence on $\phi \in [0, 2\pi)$ but no dependence on z, r or time. In this setup $r > a$, so we have the potential $A_\phi = \Phi/2\pi r$. The time-independent Hamiltonian is:

$$H = \frac{1}{2m}(\hat{p} + \frac{e}{c}A_\phi)^2 = \frac{1}{2mr^2}\left(-i\hbar\frac{\partial}{\partial\phi} + \frac{e\Phi}{2\pi c}\right)^2 \tag{8}$$

Our energy eigenstates respect the periodic boundary condition on ϕ:

$$\psi_n = \frac{1}{\sqrt{2\pi r}}e^{in\phi}, \quad n \in \mathbb{Z} \tag{9}$$

Plugging (8), (9) into the time-independent Schrödinger equation $H\psi = E\psi$, we get an energy spectrum dependent on the ratio Φ/Φ_0:

$$E = \frac{1}{2mr^2}\left(\hbar n + \frac{e\Phi}{2\pi c}\right)^2 = \frac{\hbar^2}{2mr^2}\left(n - \frac{\Phi}{\Phi_0}\right)^2 \tag{10}$$

The smooth change of the Hamiltonian (8) under a change of Φ is a phenomenon known as *spectral flow*. The energy eigenstates (9) morph into each other by periodicity – so as $\Phi \to \Phi \pm \Phi_0$, $n \to n \mp 1$ leaving the energy spectrum (10) unchanged. The presence of the solenoid's flux can only be detected for fractional values of Φ/Φ_0.

Recall the adiabatic theorem allows us to approximate the wavefunction at a time T, with an error that goes to

$1/T^2$. If we think of (9) as an instantaneous eigenstate, then the wavefunction can be expressed as [1]:

$$|\Psi(t)\rangle \simeq e^{i\theta_n(t)} e^{i\gamma_n(t)} |\psi_n(t)\rangle$$

Within the adiabatic framework, $\theta_n(t)$ is a *dynamic* phase and $\gamma_n(t)$ is a *geometric* phase. Dynamic phases apply even for stationary states, so we are interested in calculating the geometric phase – also called Berry phase. This phase arises due to *holonomy*, which is a geometric phenomenon in which a parallel transport of vectors fail to coincide after moving in a closed loop. A classic example is change in the direction of swing of a Foucault pendulum after one rotation of the earth [2, 5]. Berry phase for (9) is defined as the path integral of Berry connection $\nu_n(t)$:

$$\gamma_n(t) = \int_0^t \nu_n(t')\, dt' \quad \text{where} \quad \nu_n(t) = i\langle\psi_n(t)|\dot{\psi_n}(t)\rangle$$

This integral gives the Aharonov-Bohm phase, which is in fact a special case of the Berry phase [2].

Going back to our cyclotron setup, the adiabatic approximation is well defined here as well. We can guarantee that the final energy eigenstate must lie in the same Landau level as the initial state if $T \gg \omega_c$. Looking at eqn. (7) however, we have an $\mathcal{N}$-fold degeneracy. Our eigenstate could move freely in this $\mathcal{N}$-dimensional subspace, so our Berry phase is no longer a unit complex number but a unitary matrix $U \in U(\mathcal{N})$.

$$U = \mathcal{P} \exp\left(\oint \nu_i(\lambda_i)\, d\lambda^i\right) \tag{11}$$

U is called the *Berry holonomy* and is important in our understanding of non-Abelian quantum Hall states. Here $\mathcal{P}$ is a *path-ordering* procedure that orders a product of operators according to the value of chosen parameter λ_i. This ensures that the exponential encodes the holonomy of the Berry connection ν_i.

We define the gauge invariant curl of Berry connection $\mathbf{D}_n(\lambda) \equiv \nabla_\lambda \times \nu_n(\lambda)$ as *Berry curvature*. We have:

$$\int \mathbf{D}_i(\lambda_i)\, d\lambda^i = 2\pi C \tag{12}$$

The integer $C \in \mathbb{Z}$ is called the *Chern number*.

II. Integer Quantum Hall Effect

Klaus von Klitzing [6] discovered the quantization of Hall conductance in his 1980 experiment which used a silicon MOSFET (metal-oxide-semiconductor field effect transistor) under a strong magnetic field of order 15 Tesla.

When ν Landau levels are filled we get $\rho_{xy} = 2\pi\hbar/e^2\nu$. Continuing our calculation in the Drude model, we expect the Hall conductivity should depend on the density of electrons d: $\rho_{xy} = B/de$. Combining these two expressions, we see that the density required to fill ν Landau levels in Fig. 4, landing us in the ν^{th} plateau: $d = \frac{B}{\Phi_0}\nu$.

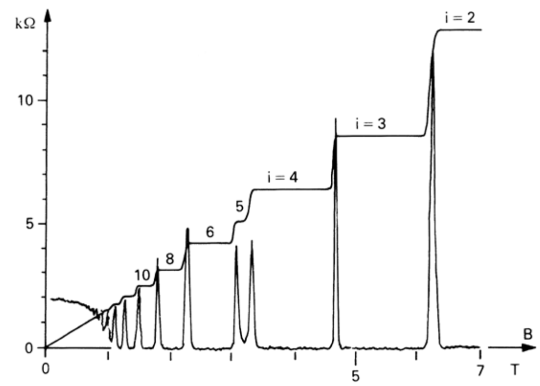

Figure 4: Integer quantum Hall effect with $\nu \in \mathbb{Z}$. Even in a disordered sample, we see the transverse Hall resistivity ρ_{xy} exhibiting plateaus while the longitudinal resistivity ρ_{xx} vanishes.

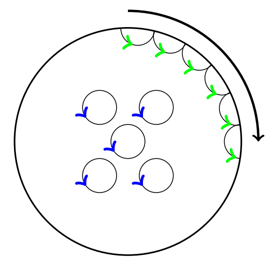

Figure 5: Bulk states (blue) and edge states (green). Edge current is oriented opposite to the cyclotron orbit.

At the ν^{th} plateau, we have the energy gap $\Delta = \hbar\omega_c$ to fill the next Landau level. A small electric field would simply tilt the spectrum, but would not cause any electrons to occupy the next level. The material effectively acts like an insulator and explains the behavior $\rho_{xx} = 0$.

A. Edge Modes

We have seen the role of geometry in describing the Berry phase (11), and now we will see the effects of topology. The states of our particle in a particular Landau level can complete their orbit in the bulk of the sample and have a fixed orientation given by the direction of $\mathbf{B}$. However at the edge, the states cannot complete their orbits and collide with the boundary. They must also maintain the same orientation as the bulk states. This is an example of *bulk-boundary correspondence*, a familiar theme that also shows up in string theory.

Fig. 5 shows how edge states propagate by bouncing off the boundary to produce an overall current that has the opposite orientation. Such a particle restricted to move along a particular line is *chiral*. According to the Nielsen-Ninomiya theorem [7], the existence of chiral fermions in a one-dimensional BZ is prohibited. However, our system has a two-dimensional boundary which does not violate the theorem. Because of the dependence of the current on the boundary, such a material is called a *topological insulator*.

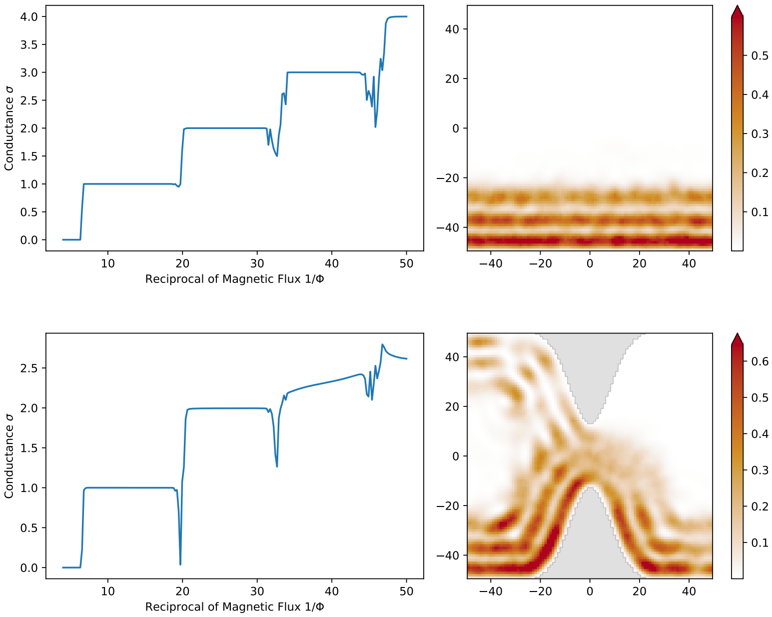

Figure 6: Numerical simulations of the quantum Hall effect using [8]. Left column is a conductance plot, right column is a heatmap of density of states. Top row is a perfect simulation with quantization of conductance. Bottom row shows effects of disorder around $1/\Phi = 40$, where the third plateau fails to occur due to partial backscattering.

B. Disorder

Any impurities present in the sample will introduce *disorder*, which turns out to be important to describing the plateaus in conductivity. We can model these as random fluctuations of the Hamiltonian in the form of peaks and troughs in the by adding a $V(\mathbf{x})_{\text{dis}}$ potential. Here we define *extended* states as spread throughout the system, these are the familiar cyclotron orbits with a fixed translated center. Disorder broadens the Landau levels and gives us a new notion of *localized* states, which are moving in equipotential lines. Only the extended states contribute to conductivity, because only they allow charge mobility across the sample. A simulation of disorder can be seen in Fig. 6

It was shown by Laughlin [9] that the integer quantum Hall effect is intimately related to the extended nature of the states near the center of the disorder-broadened Landau level. Edge effects – like shown in Fig. 5 – do not influence the accuracy of the quantization.

The potential $V(\mathbf{x})$ must obey the following conditions:

$$V_{\text{dis}} \ll \Delta\,,\ |\nabla V_{\text{dis}}| \ll \frac{\hbar\omega_c}{l_B} \quad \text{where} \quad l_B = \sqrt{\frac{\hbar}{m\omega_c}} \tag{13}$$

This means that our potential fluctuations must be smooth relative to the magnetic length l_B, which is the length scale of the oscillator. However $V(\mathbf{x})$ must be a weak perturbation or we fail to maintain discrete Landau levels. So, we need the right amount of disorder to satisfy these conditions.

For the plateaus to occur, we also need constant σ over a range of $\mathbf{B}$. We can explain this given our distinction of the states. While increasing $\mathbf{B}$, we first fill the extended states in a given Landau level, then the localized states. We observe plateaus because the localized states do not contribute to conductivity.

Consider the setup of a metal disk with a hole cut out at the center (annulus) and a solenoid passing through it. We will see how spectral flow is affected by disorder [4]. We use polar coordinates because of the additional r dependence and tweak the Hamiltonian from (8):

$$H_\Phi = \frac{1}{2m}\left[-\hbar^2 \frac{1}{r}\frac{\partial}{\partial r}\left(r\frac{\partial}{\partial r}\right) + \left(-\frac{i\hbar}{r}\frac{\partial}{\partial\phi} + \frac{eBr}{2} + \frac{e\Phi}{2\pi r}\right)^2\right] + V_{\text{dis}}(r,\phi)$$

The flux Φ affects only the extended states, and leaves localized states unchanged. This is because only extended states undergo spectral flow and map onto themselves.

C. Kubo Formula and TKNN Invariant

In this section we look at the *Kubo formula* which gives us the off-diagonal components of our Hall conductivity tensor (5) and how it relates to the Chern number (12). We need tools from quantum mechanics and topology.

We treat the electric current as a perturbation to the original Hamiltonian (8). So the overall Hamiltonian is $H = H^{(0)} + \Delta H$ with $\Delta H = -\mathbf{J}A\cdot\mathbf{A}$ with current density $\mathbf{J}$ and current $\mathbf{J}A$. The ground state of the system is $|\psi_o\rangle$.

To prove the Kubo formula from kinetic theory [4]:

- Use time-dependent perturbation theory to find $\langle\mathbf{J}(t)\rangle$ which depends on ω. We discard higher order, assuming system responds only to the linear term.
- Take $\omega \to 0$ for DC current.
- Work within a temperature limit $T \to 0$.

The Kubo formula for Hall conductivity becomes:

$$\sigma_{xy} = i\hbar A \sum_{n\neq\psi_0} \frac{\langle\psi_0|J_y|n\rangle\langle n|J_x|\psi_0\rangle - \langle\psi_0|J_x|n\rangle\langle n|J_y|\psi_0\rangle}{(E_n - E_0)^2}$$

A (flat) torus can be thought of in two ways: a rectangle of area $A = L_x L_y$ with oriented edges and a circle bundle over a circle. We let the torus have two fluxes – Φ_x and Φ_y – going through each circle. As seen from (9) these flux parameters should be periodic. So the parameter space is a torus, namely $\mathbf{T}^2_\Phi$, parametrized by dimensionless angle $\theta_i = 2\pi\Phi_i/\Phi_0$. Rewriting the Kubo formula:

$$\sigma_{xy} = i\hbar \underbrace{\left[\frac{\partial}{\partial\Phi_y}\langle\psi_0|\frac{\partial\psi_0}{\partial\Phi_x}\rangle - \frac{\partial}{\partial\Phi_x}\langle\psi_0|\frac{\partial\psi_0}{\partial\Phi_y}\rangle\right]}_{\text{Berry curvature}} \tag{14}$$

The bracketed term in (14) is $\mathbf{D}_{ij}(\Phi)$ – the curl of Berry connection $\nu_i(\Phi) = -i\langle\psi_0|\frac{\partial}{\partial\theta_i}|\psi_0\rangle$. We could think of the brackets as the curvature averaged over all fluxes.

Integrating over $\mathbf{T}^2_\Phi$ and changing variables $\Phi_i \to \theta_i$:

$$\sigma_{xy} = -\frac{e^2}{\hbar c}\int_{\mathbf{T}^2_\Phi} \frac{d^2\theta}{(2\pi)^2}\mathbf{D}_{ij}(\theta)$$

Comparing this with (12), we arrive at quantization of the Hall conductance (sign can be changed by $\mathbf{B} \to -\mathbf{B}$). We must make some assumptions about the experimental quantum Hall system:

- In $\mathbf{k}$-space on a lattice, the spectrum forms into bands. The wavefunction for each band is given by Bloch's theorem [2]: $\psi_{\mathbf{k}}(\mathbf{x}) = e^{i\mathbf{k}\cdot\mathbf{x}}u_{\mathbf{k}}(\mathbf{x})$ where $u_{\mathbf{k}}(\mathbf{x})$ is periodic over a unit cell.
- The particles do not interact with one another. In our case, electrons obey Pauli exclusion principle so they give us a multi-particle spectrum by filling up single-particle bands.
- We have the Fermi energy E_F in a *band gap*, like the insulator in Fig. 2 (right).

These assumptions ensure that each band is composed of a two-dimensional BZ which has the topology $\mathbf{T}^2 \cong \mathbf{T}^2_\Phi$. This denotes a *homeomorphism* between the two spaces, i.e there is a continuous bijective mapping between them.

So we can assign some $C_f \in \mathbb{Z}$ to each filled band, indexed by f. The TKNN formula by Thouless et al. [10] sums over all filled bands:

$$\sigma_{xy} = \underbrace{\frac{e^2}{2\pi\hbar c}C}_{\mathbf{T}^2_\Phi} = \underbrace{\frac{e^2}{2\pi\hbar c}\sum_f C_f}_{\mathbf{T}^2} \tag{15}$$

where $C = \sum_f C_f$ is a *TKNN invariant*.

D. Hofstadter Butterfly

If the flux ratio Φ/Φ_0 is a rational number $p/q \in \mathbb{Q}$ then we have a *magnetic BZ* in which the spectrum is well defined, with q gaps for E_F to be placed. Our argument for spectral flow (10) posits that we are allowed to try any real $\mathbb{R}$. This is an uncountable infinity of points for the flux ratio. Hofstadter [12] discovered that choosing irrational numbers $\mathbb{R} \setminus \mathbb{Q}$ results in a fractal pattern – a *Cantor set* – that has measure zero. Numerical simulation of the Hofstadter butterfly is shown in Fig. 7, and recently on superconducting qubit quantum computers [13].

III. Fractional Quantum Hall Effect

Previously our usage of the Drude model (3) and TKNN formula (15) was predicated on the assumption that electron interactions were negligible enough to be ignored. Starting in 1982, a surprising string of discoveries by Tsui, Störmer, et al. [14] revealed first a fraction filling factor $\nu = \frac{1}{3}$ in the lowest Landau level, then $\frac{1}{2}$, followed by many rational values for ν including even-valued denominators [15]. Fractional ν is also observed in higher Landau levels. We shall see explanations for both ground and excited states.

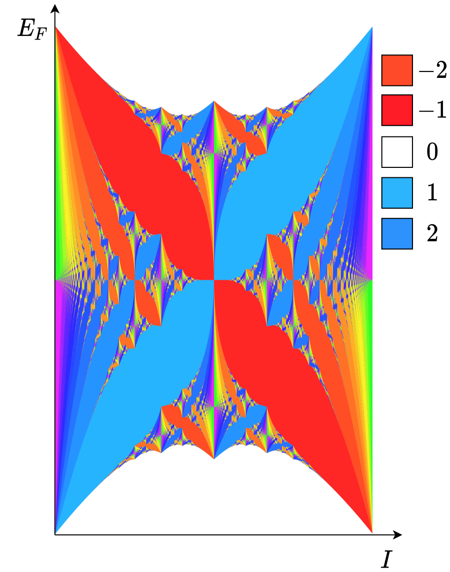

Figure 7: Hofstadter butterfly phase diagram from [11]. Colors indicate the prominent quantum Hall phases labelled by their Chern numbers. The chemical potential E_F (Fermi energy) fixes the density of the electrons. The phase is periodic in quantum flux I (magnetic flux per unit cell).

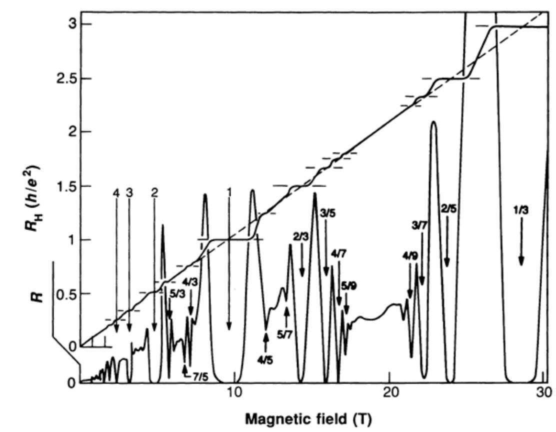

Figure 8: Fractional quantum Hall effect with $\nu \in \mathbb{Q}$. Clean samples reveal filling factor ν taking fractional values.

In our analysis we account for Coulomb interactions V_c between electrons which lifts the large degeneracy $\mathcal{N}$ (7) and also consider the disorder (13) in the material. To avoid energy crossing between Landau levels, we can make the assumption:

$$\Delta \gg V_c \gg V_{dis} \quad \text{where} \quad V_c = \frac{e^2}{|\mathbf{r}_i - \mathbf{r}_j|}$$

A. Laughlin Wavefunction for Ground States

Robert B. Laughlin provided a simple ansatz for the ground state of the quantum Hall system [9, 16] ie. the lowest Landau level where filling fraction $\nu = \frac{1}{q}$. By working in the symmetric gauge, we can treat them as eigenstates of the angular momentum operator $\hat{J}_z$. So $\psi_q \sim z^q e^{-|z|^2}$ where $z \equiv \frac{1}{\sqrt{2m}l_B}(x+iy)$ and $\hbar q$ is the eigenvalue of $\hat{J}_z$. The Laughlin wavefunction for N identical particles is given by the formula:

$$\psi_q(z_1, z_2, \ldots, z_N) = A \underbrace{\left[\prod_{i<j}^{N}(z_i - z_j)^q\right]}_{f(z_i)} \exp\left(-\frac{1}{2}\sum_{i}^{N}|z_i|^2\right) \tag{16}$$

When $q = 1$, this wavefunction describes electrons because the $f(z_i)$ term follows the *symmetrization axiom* – exchanging identical fermions $z_i \leftrightarrow z_j$ introduces a minus sign – which means we do not violate Pauli exclusion [2]. We can use the *Slater determinant* to verify the Laughlin ansatz for $q = 1$:

$$\begin{vmatrix} \psi_1(z_1) & \psi_1(z_2) & \ldots & \psi_1(z_N) \\ \psi_1(z_1) & \psi_1(z_2) & \ldots & \psi_1(z_N) \\ \vdots & & \ddots & \vdots \\ \psi_1(z_1) & \psi_1(z_2) & \ldots & \psi_1(z_N) \end{vmatrix} = f(z_i)$$

The Laughlin state ψ_q (16) is a new phase of matter that is characterized by *topological order*. By changing the topology of the manifold, the degeneracy in the ground state changes. This can be seen by placing the states on a compact manifold, like a torus. We see that the ground state becomes q-fold generate. In general, a genus-g Riemann surface has degeneracy q^g.

$q > 0 \in \mathbb{Z}^+$ can take odd values which are fermions, or even values which is a bosonic quantum Hall state. When $q = 1$, ψ_q completely describes the lowest Landau level, which consists of N non-interacting fermions ($\forall\, N$). When $q > 1$, ψ_q can be written as a sum of Slater determinants. For low odd values $q = 3$ or 5, the quantum Hall fluid looks like a liquid phase of electrons. At $q > 70$, by numerical prediction the fluid crystallizes into a solid.

q is used here as a label to denote state ψ_q with $\nu = \frac{1}{q}$, but we can draw a connection to the familiar electric charge q. We can calculate the average density for the quantum Hall droplet $\langle\psi_q|\hat{d}(z)|\psi_q\rangle$ using the density operator $\hat{d}(z) \equiv \sum_{i=1}^{N}\delta(z - z_i)$. We will recover the potential for a plasma of charged particles moving in two-dimensions [4]. This is given by a Coulomb term and a background term, which try to neutralize each other. Each particle in the Coulomb term carries electric charge q.

B. Excited States

Plateaus at higher Landau levels are explained by *charged excitations*, of which there are two types: quasi-holes and quasi-particles. Charged excitations carry fractional charge, which means they obey fractional statistics From the symmetrization axiom, if we swap the positions of two identical particles the wavefunctions should differ by at most a phase:

$$\psi(\mathbf{x}_1, \mathbf{x}_2) = e^{i\phi}\psi(\mathbf{x}_2, \mathbf{x}_1) \implies \phi = \pi\alpha$$

If we swap them back again, $\phi \to 2\pi\alpha$. Bosons have $\alpha = 0$, fermions have $\alpha = 1$. We can now define *anyons* – the charged excitations in our quantum Hall setup – as particles where $\alpha \mod 2 \neq 0$ or 1. In two-dimensions, α has a sign that denotes whether we wound the particles clockwise or anti-clockwise.

Quasi-holes/quasi-particles have a positive/negative charge $q^*_\pm = \pm e/q$, these were measured by quantum shot noise experiments [17], and recently in 2020 [18]. In our spectral flow argument (10), as we increase Φ from 0 to Φ_0a quasi-particle of charge q^*_- is transferred from the inner ring to the outer ring of the annulus. This means a whole electron is transferred only when the flux is increased by $q\Phi_0$.

We can prove the fractional charge and statistics in the two-dimensional system containing M quasi-holes. This is done by transporting the anyon in an adiabatic loop C around the system. Denoting the position of the anyon by $\eta \in \mathbb{C}$, we get two Berry connections over the parameter space – holomorphic and anti-holomorphic. The holomorphic ν_{η_i} is:

$$\nu_{\eta_i} = \underbrace{-\frac{i}{2q}\sum_{j\neq i}\frac{1}{\eta_i - \eta_j} + \underbrace{\frac{i\bar{\eta}_i}{4ml_B^2}}_{\text{Charge}}}_{\text{Statistics}} \tag{17}$$

Complex conjugation gives us the corresponding $\nu_{\bar{\eta}_i}$.

The anyon's adiabatic path C must enclose some flux Φ but it does not have to enclose the other anyons. If C does not enclose other anyons, only the second term in (17) will contribute, and the Berry phase is the familiar Aharonov-Bohm phase. This implies fractional charge:

$$e^{i\gamma} = \exp\left(-i\oint_C \nu_\eta\, d\eta + \nu_{\bar{\eta}}\, d\bar{\eta}\right),\ \gamma = \frac{e\Phi}{q\hbar} \implies q^*_+ = \frac{e}{q}$$

On the other hand if C encloses one other anyon, both terms in (17) will contribute. We may think of the anyon circling around the other as two swaps $(i,j) \to (j,i) \to (i,j)$. This implies fractional statistics:

$$e^{i\gamma} = \exp\left(-\frac{1}{2q}\oint_C \frac{d\eta_1}{\eta_1 - \eta_2} + \text{h.c.}\right) = e^{i2\pi/q} \implies \alpha = \frac{1}{q}$$

For a fully filled Landau level, with $q = 1$, the quasi-holes are fermions and we get integer quantization. But for a fractional quantum Hall state, the quasi-holes are anyons.

In general, moving a quantum particle in a loop C can be formulated as a unitary operator in the Hilbert space $\mathbb{C}^2$. In two-dimensions, the anyon exchange $(i,j) \to (j,i)$

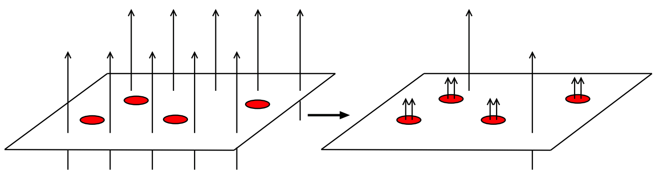

Figure 9: Image sourced from [20]. Left: Traditional picture, Right: Composite fermions

can be visualized as a braid knot of the particle world lines that cannot be unknotted. If exchange starting with anyon i or j makes no difference to the geometric phase, then we call these *abelian* anyons. Abelian anyons are the ones responsible for the fractional quantum Hall effect. Non-abelian anyons are an exotic phase of matter used in topological quantum information [19].

C. Composite Fermions

We can get the plateaus of the fractional quantum Hall effect with a slightly different reasoning. A *vortex* is the fixed angular dependence required to describe the winding nature of a wavefunction. Specifically if we have the product $f(z_i)$ from (16), fixing z_j to some position $\lambda \in \mathbb{C}$. This means simply that (16) has a zero of order q at $z = \lambda$. With abelian anyons, it does not matter if λ is fixed and z is moving or vice versa, we get the same Berry phase.

With odd values of q, we define a *composite fermion* as an electron bound to $q-1$ vortices. Lumping both of them together gives rise to one fermion. The composite fermion theory from Jain [21], says that electrons manage to space themselves out by associating with these vortex-like excitations [20]. If we have have a density d of composite fermions, they experience a different magnetic field B^* and filling factor ν^*. Our approach gives rise to the following result:

$$\gamma = \frac{2\pi A B^*}{\Phi_0} \quad \text{where} \quad B^* = B_z - (q-1)\Phi_0 d \quad \text{and}$$

$$d = \frac{\nu^* B^*}{\Phi_0} = \frac{\nu B_z}{\Phi_0} \implies \nu = \begin{cases} \frac{\nu^*}{1+(q-1)\nu^*}, & B^* > 0 \\ \frac{\nu^*}{(q-1)\nu^*-1}, & B^* < 0 \end{cases}$$

If we fill the lowest Landau level with composite fermions we get back $\nu = \frac{1}{q}$. So, the fractional quantum Hall effect emerges from the integer quantum Hall effect for composite fermions.

For even $q = 2$, or $\nu = \frac{1}{2}$, we get a striking prediction. According to (16) this describes bosons, but in the composite fermion picture it describes a half filled ground state. We predict $B^* = 0$ which means this composite fermion does not experience the **B** field.

The composite fermion unites the integer and fractional quantum Hall effects by successfully predicting the plateaus to either side of $\nu = \frac{1}{2}$, all we need to do is appropriately tune the magnetic field.

Acknowledgments

Many thanks to MIT and edX for making this course and others available to anyone for no cost. Special thanks to Prof. Barton Zweibach for his lively explanations and Mark Weitzman for helping out the edX community.

[1] B. Zwiebach, "Lecture Notes on Quantum Physics: 8.04, 8.05, 8.06,". `https://ocw.mit.edu/`.

[2] D. J. Griffiths, *Introduction to Quantum Mechanics*. Cambridge University Press, 2020.

[3] E. H. Hall, "On a new action of the magnet on electric currents," *American Journal of Mathematics* **3** (1879) .

[4] D. Tong, "Lectures on Theoretical Physics,". `https://www.damtp.cam.ac.uk/user/tong/teaching.html`.

[5] Wilczek and Shapere, *Geometric Phases in Physics*.

[6] K. v. Klitzing *et al.*, "New Method for High-Accuracy Determination of the Fine-Structure Constant Based on Quantized Hall Resistance," *Phys. Rev. Lett.* **45** (1980) .

[7] H. Nielsen and M. Ninomiya, "A no-go theorem for regularizing chiral fermions," *Physics Letters B* **105** .

[8] C. W. Groth *et al.*, "Kwant: a software package for quantum transport," *New Journal of Physics* **16** no. 6, .

[9] R. B. Laughlin, "Quantized Hall conductivity in two dimensions," *Phys. Rev. B* **23** (1981) 5632–5633.

[10] D. J. Thouless *et al.*, "Quantized Hall Conductance in a Two-Dimensional Periodic Potential," *Phys. Rev. Lett.* **49** (1982) 405–408.

[11] J. E. Avron *et al.*, "Top. quantum numbers in the Hall effect,". `https://arxiv.org/abs/math-ph/0303055`.

[12] D. R. Hofstadter, "Energy levels and wave functions of Bloch electrons in rational and irrational magnetic fields," *Phys. Rev. B* **14** (1976) 2239–2249.

[13] P. Roushan *et al.*, "Spectroscopic signatures of localization with interacting photons in superconducting qubits," *Science* **358** (2017) no. 6367, 1175–1179.

[14] D. C. Tsui *et al.*, "Two-Dimensional Magnetotransport in the Extreme Quantum Limit," *Phys. Rev. Lett.* **48** .

[15] R. Willett *et al.*, "Observation of an even-denominator quantum number in the fractional quantum Hall effect," *Phys. Rev. Lett.* **59** (1987) 1776–1779.

[16] R. B. Laughlin, "Anomalous Quantum Hall Effect: An Incompressible Quantum Fluid with Fractionally Charged Excitations," *Phys. Rev. Lett.* **50** (1983) .

[17] R. de Picciotto *et al.*, "Direct observation of a fractional charge," *Physica B: Condensed Matter* **249-251** (1998) .

[18] J. Nakamura *et al.*, "Direct observation of anyonic braiding statistics," *Nature Physics* **16** (2020) no. 9, .

[19] J. Preskill, "PH 219/CS 219 Lecture Notes,". `http://theory.caltech.edu/~preskill/ph229/`.

[20] A. Akhmerov *et al.*, "Online course on topology in condensed matter,". `https://topocondmat.org`.

[21] J. K. Jain, "Composite-fermion approach for the fractional quantum Hall effect," *Phys. Rev. Lett.* **63** .